

Directed connectivity of brain default networks in resting state using GCA and motif

Zhuqing Jiao^{1,2}, Huan Wang¹, Kai Ma¹, Ling Zou^{1,2}, Jianbo Xiang^{2,3}

¹School of Information Science and Engineering, Changzhou University, Changzhou 213164, China,

²Changzhou Key Laboratory of Biomedical Information Technology, Changzhou University, Changzhou

213164, China, ³Department of Medical Imaging, Changzhou No.2 People's Hospital Affiliated with Nanjing Medical University, Changzhou 213003, China

TABLE OF CONTENTS

1. Abstract
2. Introduction
3. fMRI Data Processing
4. GCA and Motif Structure
5. Experimental Analysis
6. Conclusions
7. Acknowledgements
8. References

1. ABSTRACT

Nowadays, there is a lot of interest in assessing functional interactions between key brain regions. In this paper, Granger causality analysis (GCA) and motif structure are adopted to study directed connectivity of brain default mode networks (DMNs) in resting state. Firstly, the time series of functional magnetic resonance imaging (fMRI) data in resting state were extracted, and the causal relationship values of the nodes representing related brain regions are analyzed in time domain to construct a default network. Then, the network structures were searched from the default networks of controls and patients to determine the fixed connection mode in the networks. The important degree of motif structures in directed connectivity of default networks was judged according to p-value and Z-score. Both node degree and average distance were used to analyze the effect degree an information transfer rate of brain regions in motifs and default networks, and efficiency of the network. Finally, activity and functional connectivity strength of the default brain regions are researched according to the change of energy distributions between the normals and the patients' brain regions. Experimental results demonstrate that, both normal subjects and stroke patients have some corresponding fixed connection mode of three nodes, and the efficiency and power spectrum of the patient's default network is somewhat lower than that of the normal person. In particular, the Right Posterior Cingulate Gyrus (PCG.R) has a larger change in functional connectivity and its activity. The research results verify the feasibility of the application of GCA and motif structure to study the functional connectivity of default networks in resting state.

2. INTRODUCTION

Nowadays default mode networks (DMNs) which are concerned most have become research hotspots of mental and neurological disorders as well as cognitive neuroscience in studying resting-state functional brain networks (1). Latterly, researchers used functional magnetic resonance imaging (fMRI) technology to study the metabolic process of brain complex systems (2), and found that default networks were closely related to the brain diseases caused by various brain abnormalities (e. g. Attention Deficit Hyperactivity Disorder (ADHD), Schizophrenia, and Alzheimer's disease, etc. (3, 4)). Uddina *et al.* (5) found in the study of network homogeneity, the default networks of ADHD patients has homogeneity decreased in Precuneus, and this kind of abnormal functional connection can cause some related attention defects or working memory obstacles, etc. Jang *et al.* (6) suggested that the functional connectivity abnormalities of default networks have high risks of schizophrenia, which may be related to the dysfunction of Anterior Cingulate Cortex and Precuneus. Hafkemeijer *et al.* (7) found that the functional connectivity of multiple brain regions was negatively correlated with age. Until now, the functional connectivity of brain regions has become a focus on studying brain science with continuous deepening of default network research.

In diagnosing the functional connectivity in default networks, if the time series of a brain region can be predicted by the current value and the past value of the time series of another brain region via a linear model, it is considered that there is a causal

relationship between the two time series. After causality test is made on the time series of related brain regions by using Granger causality test, the default network can be built by quantifying the connection strengths between nodes in brain networks (8). A motif consists of a few nodes in a network, with the size between network individuals and communities, is one of the basic network topologies (9, 10). Motif structure can reflect the structural characteristics of the default network from a much smaller range by analyzing the structure of the function of the default network. It is helpful to identify the functional differences between patients' and control's default networks in resting state. In this paper, connectivity characteristics of brain default networks are analyzed using GCA and model structure to determine the fixed connection mode of nodes in the network and study the characteristics of nodes and network efficiency. Furthermore, activity and functional connectivity strength of the default brain regions are researched according to the change of energy distributions within a specific frequency range (0.01~0.08Hz) between the normals and the patients' brain regions.

3. FMRI DATA PROCESSING

Functional connectivity can be used to test whether there is interaction information between two brain regions, which emphasizes the description of the neural activity in a brain (11). The specific steps of fMRI data processing to build a brain default network are as follows:

- (1) The original fMRI data is processed via time correction, spatial registration, normalization, and smoothing, etc. (12). The whole brain time series data are obtained by filtering high-frequency physiological noise and low frequency signals. Filtering range is 0.01~0.08Hz (13).
- (2) The whole brain is divided into 90 brain regions (The left and the right brains are divided into 45 regions respectively) according to Automatic Labeling Anatomical (AAL) template. Each node in the brain network represents a separate brain region.
- (3) Granger causality analysis is conducted to obtain the significant degree of the causal relationships between nodes in the network by using the time series of the default brain regions.
- (4) Adjacency Matrix \mathbf{A} is adopted to describe the connections between nodes. If there is a causal relationship between the nodes, the value of the element in the corresponding location is set to 1; otherwise, 0. Matrix diagonal elements are set to 0 in order to avoid the appearance of self-connected edges in the network.

By the above steps, a default network can be formed by default brain regions, while the number of random connections in the network is minimized.

4. GCA AND MOTIF STRUCTURE

Granger causality test is a common method to study the causal relationship between variables on the base of causality of time series. When defining connectivity and connection way between brain regions in brain networks, it is unnecessary to assume the state hypothesis, and the results of causal relationships are reflected in the form of prediction (14, 15).

If the time series of node \mathbf{X} and node \mathbf{Y} are expressed x_t and y_t respectively, the regression model with two variables in time domain is considered as (16):

$$x_t = \sum_{i=1}^{\infty} A_{1i} x_{t-i} + a_{1t} \quad (1)$$

$$y_t = \sum_{i=1}^{\infty} B_{1i} y_{t-i} + b_{1t} \quad (2)$$

where a_{1t} , b_{1t} are the predictor error terms, $D(a_{1t}) = U_1$ and $D(b_{1t}) = V_1$ are the variances of the error term.

By Esq. (1) and Esq. (2), the states of node \mathbf{X} or node \mathbf{Y} at time t can be estimated by their own past states. Considering the mutual relation between variables, the regression models of node \mathbf{X} and node \mathbf{Y} are as follows:

$$x_t = \sum_{i=1}^{\infty} A_{2i} x_{t-i} + \sum_{i=1}^{\infty} B_{2i} y_{t-i} + a_{2t} \quad (3)$$

$$y_t = \sum_{i=1}^{\infty} C_{2i} x_{t-i} + \sum_{i=1}^{\infty} D_{2i} y_{t-i} + b_{2t} \quad (4)$$

where $D(a_{2t}) = U_2$ and $D(b_{2t}) = V_2$ are the variances of error terms.

The roles of \mathbf{Y} on \mathbf{X} and \mathbf{X} on \mathbf{Y} are respectively defined as:

$$F_1 = \ln(U_1/U_2) \quad (5)$$

$$F_2 = \ln(V_1/V_2) \quad (6)$$

GCA defines the direction of connectivity between brain regions. After constructing a directed connection network by using default brain regions, we can analyze the basic characteristics of the network such as node degree, average distance, etc.

A motif is defined as:

- (1) The probability, that the occurrence number in a random network corresponding to a real network is greater than the occurrence number in the real network, is very small, and generally the probability is required less than a threshold p , such as $p = 0.01$;

Table 1. Three-node motif structure

ID	0	1	2	3	4	5	6
Motif							
ID	7	8	9	10	11	12	
Motif							

- (2) The occurrence number of the sub-graph in a real network N_{real} is not less than a lower limit U ;
- (3) The occurrence number of the sub-graph in a real network N_{real} is significantly higher than the occurrence number in a random network, and generally required $(N_{real} - N_{rand}) > 0.1N_{rand}$.

Normally, importance of the motif structure in the network is measured according to the p -value, Z-score etc. (17, 18). In most networks, common motifs are composed of three nodes or four nodes. The structures of three-node motif are shown in Table 1 (19).

In order to study the functional structure of the default network from a smaller range, motifs are used to analyze local features of default networks, research network topologies, and determine the functional differences existing on default brain regions between controls and patients (20, 21). The p -value and Z-score of the motifs in the network can be obtained after the phantom is detected. The smaller p -value, the most important the motif structure composed of related nodes in the default network. The greater Z-score, the higher importance of the motif has in the default network. For Motif M_i , N_{reali} is its occurrence number in the real network, N_{randi} is its occurrence number in the random network, $\langle N_{randi} \rangle$ is the average value of N_{randi} , and σ_{randi} is the standard deviation. Then the Z-score of motif M_i in the real network is:

$$Z_i = \frac{N_{reali} - \langle N_{randi} \rangle}{\sigma_{randi}} \quad (7)$$

Degree is used to measure the effect degree of a node in motifs. It is divided into outdegree and indegree which can reflect the directed connection strength of related brain regions in the network. If there are n nodes in network G and the degree of node v_i is w_i , the outdegree and indegree of nodes are w_i^{out} and w_i^{in} , respectively. Then,

$$w_i = w_i^{in} + w_i^{out} \quad (8)$$

The greater degree, the greater effect of the node in default networks. If a node has a single outdegree or indegree, it indicates that the connection strength of the node in the network is relatively weak.

The distance between nodes in the network is helpful to study the transmission speed of information in motifs and default networks, and the average distance can describe separation degree of nodes, that is, small world effect. Define the distance d_{ij} from node v_i to node v_j as the minimum number of edges to experience from v_i to v_j , and its reciprocal $1/d_{ij}$ is called the efficiency from node v_i to node v_j , denoted as ε_{ij} , which represents the information transmission speed between two points. The average distance of the network is defined as L :

$$L = \frac{1}{N(N-1)} \sum_{i \neq j} d_{ij} \quad (9)$$

The efficiency of the network is defined as L_c :

$$L_c = \frac{1}{N(N-1)} \sum_{i \neq j} \varepsilon_{ij} \quad (10)$$

The greater distance between two nodes in a network, the smaller efficiency between the nodes and the lower efficiency of the motifs is.

5. EXPERIMENTAL ANALYSIS

A PHILIPS 3.0-Tesla scanner is utilized to collect brain fMRI data. Scanning parameters are set as follows. Functional Image: Axial Slices = 24, Layer Thickness = 4mm, Repeat Time TR = 2000ms, Echo Time TE = 35ms, angle flip = 90°, FOV = 230mm × 182mm. Structure Image: 3D Sequence Number = 270, Layer Thickness = 0.6mm, Repeat Time TR = 7.4ms, Echo Time TE = 3.4ms, Angle Flip = 8°, FOV = 250mm × 250 mm.

Experiments are performed in 15 stroke patients and 20 normal controls, all of which are carried on fMRI scanning in resting state. The patients

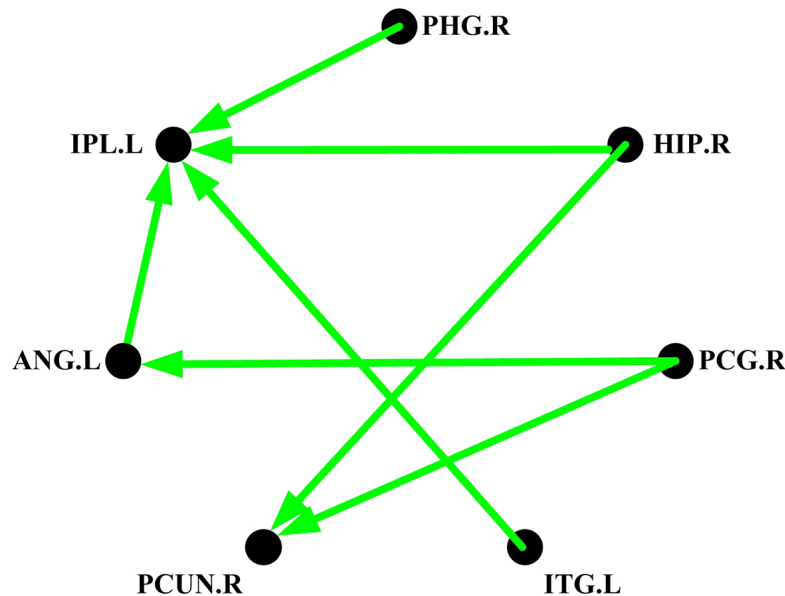


Figure 1. Default network architecture of patients.

include 9 males and 6 females, aged between 65~75 years old. Normal controls include 10 men and 10 women, aged between 18~25 years old. Prior to the acquisition of the brain fMRI data, it is indispensable to understand the physical state of the volunteers, so that subjects are examined whether the presence of metal objects, and to remind participants to stay awake and stop conscious thinking activities.

After a series of preprocessing, part of the default brain regions of patients and controls were selected to analyze by GCA repeatedly. We found the network formed by Right Posterior Cingulate (PCG.R) Right Hippocampus (HIP.R), Right Parahippocampal Gyrus (PHG.R), Left Angular Gyrus (ANG.L), Left Inferior Parietal Lobule (IPL.L), Right Precuneus (PCUN.R) and Left Inferior Temporal Gyrus (ITG.L) had relatively obvious connection characteristics. The default network structure of the patient composed of the above brain regions is shown in Figure 1.

From Figure 1, we can see that there are not only unidirectional connections, but also a bi-directional connection between the nodes. IPL.L, HIP.R and ANG.L belong to a bi-directional connection, which indicates that their functional connectivity in the patients' default network is relatively stronger. Other nodes belong to unidirectional connection, which indicates that functional connectivity of the nodes in the network is relatively weak.

PCG.R, HIP.R, PHG.R, IPL.L, ANG.L, PCUN.R, and ITG.L are numbered according to the order of 0~6. Matrix C_1 is used to describe the directed connectivity of patients' default network between the nodes, C_1 is expressed as:



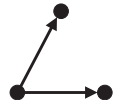

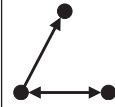
$$c_1 = [0.4; 0.5; 1.3; 1.5; 2.3; 3.1; 4.3; 6.3] \quad (11)$$

Rand-ESU algorithm in Fanmod software is used to search the type and quantity of motifs in the default network according to C_1 (22). It is helpful to determine whether there is a fixed connection mode, so as to research structural characteristics of the network from a smaller range. Since there are fewer nodes in the network, this experiment only verifies the existence of three-node motifs. The detection results are shown in Table 2.

As shown in Table 2, the p -values of the sub-graphs No. 5, No. 6, No. 0 and No. 2 are greater than 0.01, thus it may be known the sub-graphs are not the motifs of the default network. The p -value of the sub-graph No. 1 is 0, less than 0.01, and its frequency appearing in real default networks is higher than that in random networks, so that the sub-graph is a motif in default network for patients. Motif No. 1 corresponds to the nodes PCG.R, ANG.L and IPL.L, and its Z-score is 0.95071. It indicates that the directed connectivity composed of the above 3 nodes has significant effects on the default network.

Through the directed connectivity, we can study the distance between the nodes and the average distance of the constructed default networks for patients and controls, and analyze the information transmission rate and network efficiency. According to Figure 1, we can calculate the distances of node pairs (0, 1), (2, 5) and (6, 5) are 3, then there is the slowest information transmission speed between these nodes. The distances of node pairs (0, 3), (3, 5), (4, 1) and (6, 1) are 2, and the information transmission speed is relatively fast. The distances of other node pairs are 1,

Table 2. Detection results of 3-node motifs in default network of patients

ID	5	6	0	1	2
Sub-graph					
Frequency[O]	40%	30%	10%	10%	10%
Mean-Freq[R]	41.825%	30.55%	8.2625%	5.25%	8.175%
Z-Score	-0.38686	-0.1265	0.3712	0.95071	0.38686
p-Value	0.241	0.234	0.241	0	0.234

which is the fastest transmission speed. The average distance L of patients' default network is 0.5952 and efficiency of the network L_c is 0.2619 according to the distance of node pairs. The average distance of motif No. 1 is 0.6667, and the efficiency of the motif L_{c1} is 0.4167. These results indicate that the efficiency of motifs is higher than that of the default network, but the small world effect of the entire default network is more obvious.

Under the same conditions, GCA is conducted on the same default brain regions of the controls, and it is found that the default network structure of the controls is significantly different from that of the patients, as shown in Figure 2.

As shown in Figure 2, the density of the node connection of the controls is higher than that of the patients, which indicates that the functional connectivity strength of the patients' default network has decreased. PCG.R only has indegree but the maximum node degree, which indicates that the node has a significant role in the network. PCUN.R has relatively smaller node degree and its functional connectivity is relatively weak, while the function connectivity of the other nodes is strengthened. Similarly, the motifs of the default network for the controls are analyzed according to the network structure, and directed connectivity of node pairs in the default network are described by using Matrix C_2 .

$$C_2 = \begin{bmatrix} 1 & 0 & 1 & 2 & 1 & 3 & 1 & 6 & 2 & 1 & 2 & 3 & 2 & 4 & 2 & 6 & 3 & 0 & 3 & 1 & 3 & 6 & 4 & 0 & 4 & 1 & 4 & 3 & 5 & 0 & 5 & 3 & 5 & 4 & 6 & 0 & 6 & 1 \end{bmatrix} \quad (12)$$

The type and number of the motifs in the default network are determined by Matrix C_2 , as shown in Table 3.

As shown in Table 3, the p -value of sub-graphs No. 3 and No. 9 is 0, less than 0.01, and their occurrence number in true networks is higher than that in random networks. The sub-graph No. 3 and No. 9 are all the motifs of the controls' default networks. It can be seen in Figure 2, PHG.R, HIP.R and PCG.R are corresponding to sub-graph No. 9, and the Z-score of the sub-graph is 0.95071, which is relatively large. This

shows that the fixed connection between the above three nodes is important to the controls' default network. The Z-score of sub-graph No. 3 is 1.0234, and there are many groups of different node combinations in the network, which indicates that these connections play the largest role in the default network of the controls. The p -values of other sub-graphs are more than 0.01, which indicates that there is no fixed connection mode in the default networks of the controls.

The distance between the nodes in the network is calculated according to Figure 2. According to Figure 1, we can calculate that the distances of node pairs (1, 6) and (5, 2) are 3, and then there is the slowest information transmission speed between these nodes. The distances of node pairs (1, 3), (2, 0), (3, 2), (4, 6), (5, 1) and (5, 6) are 2, which shows the information transmission speed is relatively faster. The distances of the other pair nodes are 1, which indicates that the transmission speed is the fastest among the nodes. After calculation, the average distance of the controls' default network is 0.7857, and network efficiency L_c is 0.4444. The average distance of No. 9 is $L_9 = 0.6667$, and the efficiency of No. 9 is $L_{c9} = 0.6667$. The average distance of sub-graph No. 3 is $L_3 = 0.5$, and its efficiency is $L_{c3} = 0.5$. The results show that the efficiency of No. 9 is higher than that of No. 3 and the entire default network, but the average distance of No. 3 is smaller, and its small world effect is more obvious. Network efficiency of the controls is higher than that of the patients, which indicates some brain regions of patients with dysfunction. The average distance of the patients' default network is less than the controls', which indicates that the small world effect of the patient's network is more obvious.

Through diagnosing default networks of patients and controls, it is helpful to understand and recognize the functional connectivity of some related brain regions. In the controls' default network, PCG.R only has an indegree but the highest node degree, which shows that the node plays the most important roles in the network. IPL.L also has a higher degree, which indicates that the node has an important function, and the function of other nodes has a tendency to

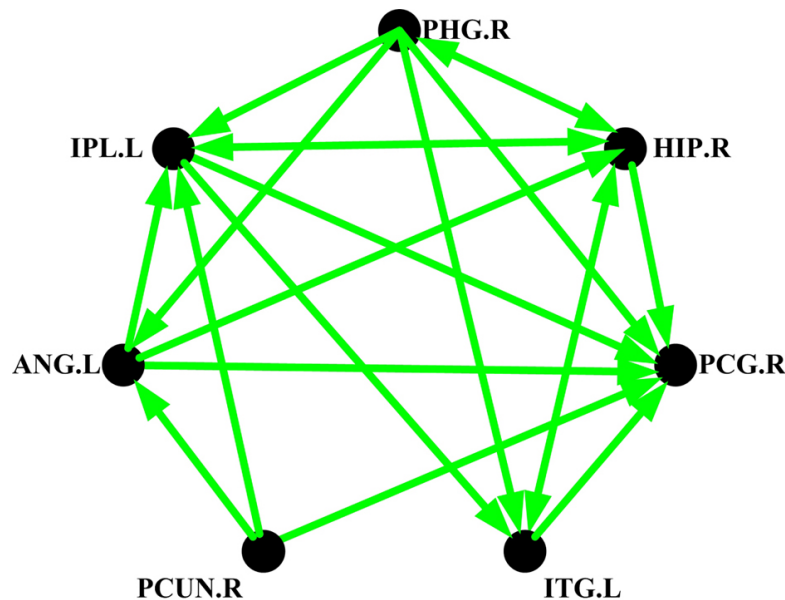


Figure 2. Default network structure for controls.

decrease in different degree. In the patients' default network, IPL.L node has the largest degree, indicating that the node in the patients' default network has played an important role.

But note that the degrees of PCG.R and PHG.R change a lot, and their functional connectivity has a greater degree of change. Other nodes have very small changes, and the role of PCG.R in the default network of the controls is the largest. This shows that PCG.R has a key role in the transformation process from normal people to the stroke patients, and other brain regions have different levels of influence. After analyzing the change of energy distribution of patients and normals at different frequencies, we can have a better understanding about the transition from normals to patients. The node for PCG.R, PHG.R, HIP.R, IPL.L, which have a higher node degree, are selected to analyze, which are the components of the default networks of the normals and the patients, as shown in Figure 3.

As seen from Figure 3, the same brain regions of different patients show different energy changes in the low frequency range. The maximum energy values of PCG.R and PHG.R of Patient 2 is much higher than in those of Patient 1, and the maximum energy values of HIP.R and IPL.L of Patient 1 have obvious difference with those of the other patient. It shows that there is obvious difference in the active degree of the same brain regions from different patients. Similarly, it is feasible to analyze the energy distribution in default networks of normal subjects in a specific frequency range, as shown in Figure 4.

As seen from Figure 4, for normal subjects, there are different characteristics of energy distribution

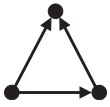


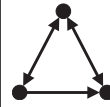
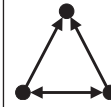

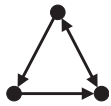

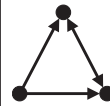
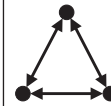
in the same brain regions in a specific frequency range. The maximum energy values of PCG.R and IPL.L of Normal 2 are greater than the other normal, the maximum energy values of their PHG.R are basically the same, but in different frequency the maximum energy values of IPL.L of normal 1 are less than those of Normal 2.

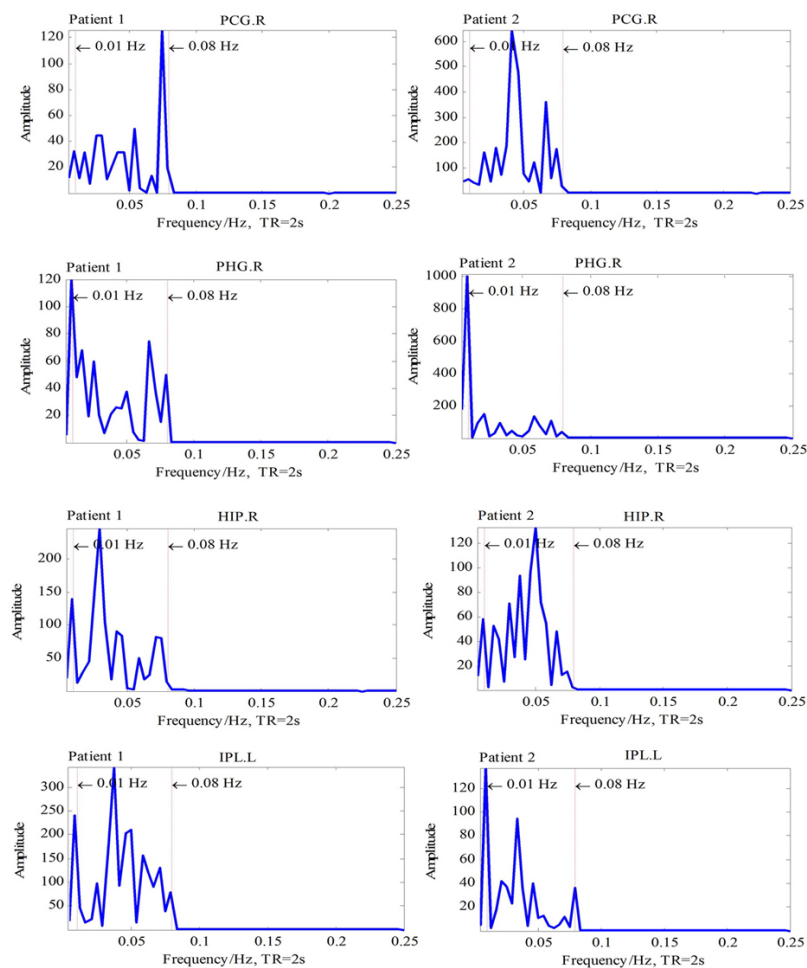
According to Figure 3 and Figure 4, we can find that, in the low frequency range of 0.01~0.08Hz, most of the energy fluctuation ranges of PHG.R, HIP.R, PCG.R and IPL.L in normals are higher than those in patients, and the maximum energy value in normals is much higher than that in patients. This shows that the activity of some brain regions in patient's default network weakened, and the intensity of functional connectivity decreased compared with the normals, which is consistent with the complexity of their default networks in resting state. In these brain regions, PCG.R has the greatest Energy variation range, indicating that it could play an important role in the transition from normals to patients.

6. CONCLUSIONS

In this paper, GCA and motif are used to analyze the functional connectivity of brain default networks in a smaller range. GCA is performed to the time series of default brain regions to construct a default network. After searching the number and types of different motifs in the network, the roles of the motifs in default networks are determined by p -value and Z-score. The transmission rate of information in the network and the efficiencies of the related motifs are obtained based on average distances between nodes,

Table 3. Detection of three-node motifs in default network of controls

ID	3	1	5	9	4
Motif					
Frequency[O]	26.667%	20%	16.667%	10%	6.6667%
Mean-Freq[R]	24.058%	17.932%	17.165%	7.4654%	7.5115%
Z-Score	1.0234	0.41941	-0.16186	1.6627	-0.36512
p-Value	0	0.289	0.577	0	0.442
ID	6	10	0	11	12
Motif					
Frequency[O]	6.6667%	3.3333%	3.3333%	3.3333%	3.3333%
Mean-Freq[R]	7.4179%	3.7588%	4.6804%	3.7071%	3.1283%
Z-Score	-0.26862	-0.20474	-0.81926	-0.3512	0.071081
p-Value	0.294	0.295	0.44	0.148	0.137

**Figure 3.** Energy distributions of some brain regions in default networks of patients.

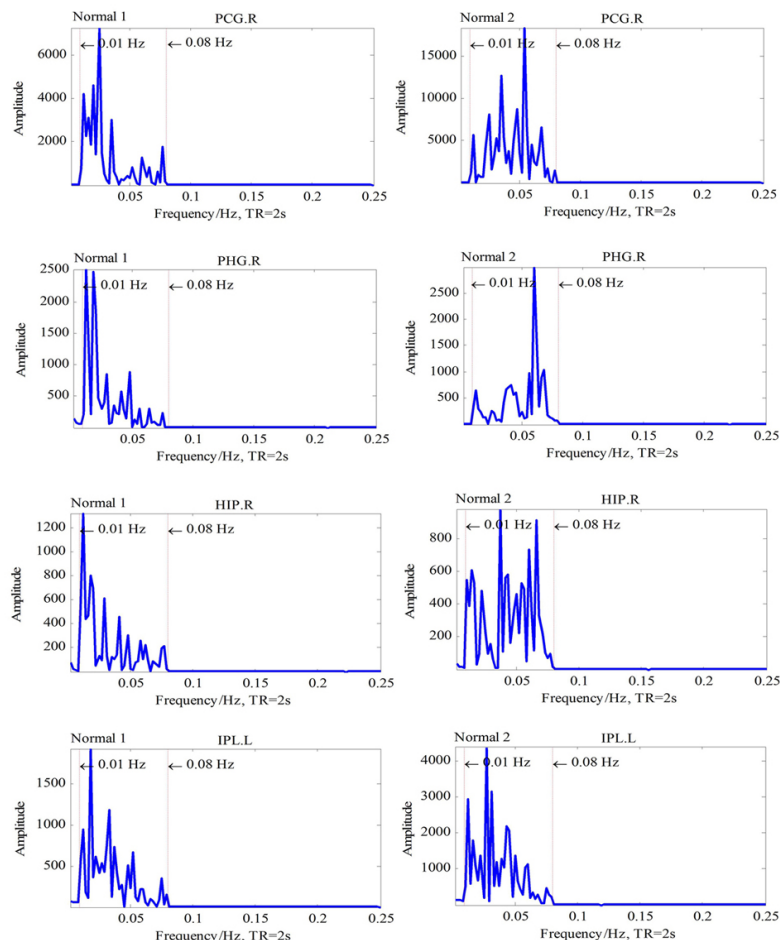


Figure 4. Energy distributions of some brain regions in default networks of normal.

and the study results of the patients were compared with those of the controls. The activity and functional connectivity strength of the default brain regions are researched according to the energy distributions in brain regions associated with default networks. Experimental results are obtained on the basis of the existing data, whether the relevant motifs are the general characteristics of the default network need to continue to be improved in the follow-up experiment.

To study the characteristics of the brain default networks of patients and controls are helpful to compare the difference between the two, which have certain reference values for the study of brain diseases, such as Alzheimer's disease (23, 24), Parkinson's diseases (25), hearing loss (26, 27) and depression (28, 29) in the future.

7. ACKNOWLEDGEMENTS

This work is supported in part by the National Natural Science Foundation of China under

Grant 51307010 and Grant 61201096, the Science and Technology Program of Changzhou City under Grant CE20145055, Qing Lan Project of Jiangsu Province.

8. REFERENCES

1. Raichle ME, MacLeod AM, Snyder AZ, Powers WJ, Gusnard DA, Shulman GL. A default mode of brain function. *Proceedings of the National Academy of Sciences*, 98(2): 676-682 (2001)
DOI: 10.1073/pnas.98.2.676
2. Zhang YD, Yang JQ, Yang JF, Liu AJ, Sun P. A novel compressed sensing method for magnetic resonance imaging: Exponential wavelet iterative shrinkage-thresholding algorithm with random shift. *International Journal of Biomedical Imaging*, 3: 1-10 (2016)
DOI: 10.1155/2016/9416435

3. Zhang YD, Dong ZC, Phillips P, Wang SH, Ji GL, Yang JQ, Yuan TF. Detection of subjects and brain regions related to Alzheimer's disease using 3D MRI scans based on eigenbrain and machine learning. *Frontiers in Computational Neuroscience*, 9: 66 (2015)
DOI: 10.3389/fncom.2015.00066
4. Zhang YD, Chen XQ, Zhan TM, Jiao ZQ, Sun Y, Chen ZM, Yao Y, Fang LT, Lv YD, Wang SH. Fractal dimension estimation for developing pathological brain detection system based on Minkowski-Bouligand method. *IEEE Access*, 4: 5937-5947 (2016)
DOI: 10.1109/ACCESS.2016.2611530
5. Uddina LQ, Kelly AMC, Bharat BB, Margulies DS, Shehzada Z, Shawc D, Ghaffaria M, Rotrosenc J, Adlerc LA, Castellanos FX, Milhama MP. Network homogeneity reveals decreased integrity of default-mode network in ADHD. *Journal of Neuroscience Methods*, 169(1): 249-254 (2008)
DOI: 10.1016/j.jneumeth.2007.11.031
6. Jang JH, Jung WH, Choi JS, Kang DH, Shin NY, Hong KS, Kwon JS. Reduced prefrontal functional connectivity in the default mode network is related to greater psychopathology in subjects with high genetic loading for schizophrenia. *Schizophrenia Research*, 127(1-3): 58-65 (2011)
DOI: 10.1016/j.schres.2010.12.022
7. Hafkemeijer A, Van DGJ, Rombouts SA. Imaging the default mode network in aging and dementia. *Biochimica et Biophysica Acta*, 1822(3): 431-441 (2012)
DOI: 10.1016/j.bbadis.2011.07.008
8. Jiao ZQ, Zou L, Qian N, Ma ZH. Causality analysis of multivariable time series using VAR model and complex network measure. *Journal of Information & Computational Science*, 10(8): 2211-2220 (2013)
DOI: 10.12733/jics20101702
9. Milo R, Shen-Orr S, Itzkovitz S, Kashtan N, Chklovskii D, Alon U. Network motifs: simple building blocks of complex networks. *Science*, 298(5594): 824-827 (2002)
DOI: 10.1126/science.298.5594.824
10. Antigueira L, Oliveira ON, Costa LDF, Nunes MDGV. A complex network approach to text summarization. *Information Sciences*, 179(5): 584-599 (2009)
DOI: 10.1016/j.ins.2008.10.032
11. Luo C, Li Q, Lai YX, Xia Y, Qin Y, Liao W, Li SS, Zhou D. Altered functional connectivity in default mode network in absence epilepsy: a resting-state fMRI study. *Human brain mapping*, 32(3): 438-449 (2011)
DOI: 10.1002/hbm.21034
12. Castro NC, Azevedo PJ. Significant motifs in time series. *Statistical Analysis & Data Mining*, 5(1): 35-53 (2012)
DOI: 10.1002/sam.11134
13. Luo YM, Li BL, Liu J. Amplitude of low-frequency fluctuations in happiness: A resting-state fMRI study. *Chinese Journal*, 60(2): 170-178 (2015)
DOI: 10.1360/N972014-00700
14. Hamilton JP, Chen G, Tomason ME, Schwartz ME, Gotlib IH. Investigating neural primacy in major depressive disorder: multivariate Granger causality analysis of resting-state fMRI time-series data. *Molecular psychiatry*, 16(7): 763-772 (2011)
DOI: 10.1038/mp.2010.46
15. Benson AR, Gleich DF, and Leskovec J. Higher-order organization of complex networks. *Science*, 353(6295): 163-166 (2016)
DOI: 10.1126/science.aad9029
16. Milo R, Itzkovitz S, Kashtan N, Levitt R, Shen-Orr S, Ayzenshtat I, Sheffer M, Alon U. Superfamilies of evolved and designed networks. *Science*, 303(5663): 1538-1542 (2004)
DOI: 10.1126/science.298.5594.824
17. Kotorowicz M. Motif based hierarchical random graphs: structural properties and critical points of an Ising model. *Condensed Matter Physics*, 14(1): 2401-2410 (2011)
DOI: 10.5488/CMP.14.13801
18. Jiao ZQ, Wang H, Ma K. The connectivity measurement in complex directed networks by motif structure. *International Journal of Sensor Networks*, 21(3): 197-204 (2016)
DOI: 10.1504/IJSNET.2016.078374
19. Ferreira LK, Busatto GF. Resting-state functional connectivity in normal brain aging. *Neuroscience & Biobehavioral Reviews*, 37(3): 384-400 (2013)
DOI: 10.1016/j.neubiorev.2013.01.017
20. Wernicke S, Rasche F. FANMOD: a tool for fast network motif detection. *Bioinformatics*, 22(9): 1152-1153 (2006)
DOI: 10.1093/bioinformatics/btl038

21. Khakabimamaghani S, Sharafuddin I, Dichter N, Koch I, Masoudinejad A. Quate Xelero: an accelerated exact network motif detection algorithm. *PLoS One*, 8(7): 295-298 (2013)
DOI: 10.1371/journal.pone.0068073
22. Barks SK, Parr LA, Rilling JK. The default mode network in chimpanzees (Pan troglodytes) is similar to that of humans. *Cerebral Cortex*, 25(2): 538-544 (2015)
DOI: 10.1093/cercor/bht253
23. Zhang YD, Wang SH. Detection of Alzheimer's disease by displacement field and machine learning. *Peerj*, 3(s1): e1251 (2015)
DOI: 10.7717/peerj.1251
24. Zhang YD, Wang SH, Phillips P, Yang, JQ, Yuan TF. Three-dimensional eigenbrain for the detection of subjects and brain regions related with Alzheimer's disease. *Journal of Alzheimer's Disease*, 50(4): 1163-1179 (2016)
DOI: 10.3233/JAD-150988
25. Onyango IG, Khan SM, Bennett JP. Mitochondria in the pathophysiology of Alzheimer's and Parkinson's diseases. *Frontiers in Bioscience - Landmark*, 22(5): 854-872 (2017)
DOI: 10.2741/4521
26. Yang M, Zhang Y, Li JW, Zou L, Lu SY, Liu B, Yang JQ, Zhang YD. Detection of left-sided and right-sided hearing loss via fractional Fourier transform. *Entropy*, 18(5): 194 (2016)
DOI: 10.3390/e18050194
27. Sinai L, Owen AM, Naci L. Mapping preserved real-world cognition in severely brain-injured patients. *Frontiers in Bioscience - Landmark*, 22(5): 815-823 (2017)
DOI: 10.2741/4518
28. Smith R, Baxter LC, Thaye JF, Lane RD. Disentangling introspective and exteroceptive attentional control from emotional appraisal in depression using fMRI: A preliminary study. *Psychiatry Research Neuroimaging*, 248(2): 431-455 (2016)
DOI: 10.1016/j.psychresns.2016.01.009
29. Hui JJ, Xi GJ, Liu SS, Li XL, Geng LY, Teng GJ, Nie BB, Shan BC, Yan J, Dong L, Reynoldsf GP, Zhang ZJ. Blood oxygen level-dependent signals via fMRI in the

mood-regulating circuit using two animal models of depression are reversed by chronic escitalopram treatment. *Behavioural Brain Research*, 311(9): 210-218 (2016)
DOI: 10.1016/j.bbr.2016.05.044

Key Words: Default Networks, Granger Causality Analysis, Motif Structure, Directed Connectivity

Send correspondence to: Ling Zou, School of Information Science and Engineering, Changzhou University, Changzhou 213164, China, Tel: 86-0519-86330558, Fax: 86-0519-86330558, E-mail: zouling@cczu.edu.cn